Journal of Hazardous Materials 436 (2022) 129211

Contents lists available at ScienceDirect

Journal of Hazardous Materials

journal homepage: www.elsevier.com/locate/jhazmat

Oil biodegradation in permeable marine sediments: Effects of benthic pore-water advection and solute exchange

Xiaolong Geng [a,b,*], Christopher H. Barker [b], Amy MacFadyen [b], Michel C. Boufadel [c], Kenneth Lee [d], Dalina L. Thrift-Viveros [b], Robert Jones [b], Caitlin O'Connor [b]

[a] Genwest Systems, Inc, Edmonds, WA 98020, USA
[b] Office of Response and Restoration, Emergency Response Division, National Oceanic and Atmospheric Administration, Seattle, WA 98133, USA
[c] Department of Civil and Environmental Engineering, New Jersey Institute of Technology, University Heights, Newark, NJ 07102, USA
[d] Department of Fisheries and Oceans, Dartmouth, Nova Scotia, B2Y4A2, Canada

HIGHLIGHTS

- Ripple-flow interactions cause benthic spatially varied oil biodegradation rate.
- Benthic oil biodegradation primarily depends on local topographic and flow patterns.
- Oil biodegradation primarily occurs in ripple troughs due to direct oxygen recharge.
- Biodegradation of benthic oil deposited uphill is slow due to anaerobic conditions.

GRAPHICAL ABSTRACT

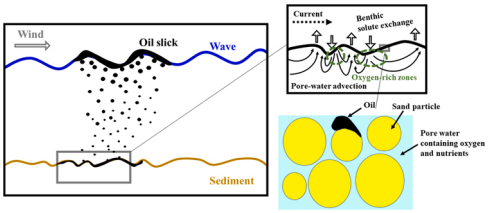

ARTICLE INFO

Editor: Jörg Rinklebe

Keywords:
Oil biodegradation
Benthic flow and solute exchange
CYL-BIOMARUN
Numerical, modeling
Sediment chamber

ABSTRACT

Oil spills have been recognized as among the worst kinds of environmental disasters, causing severe coastal ecological and economic damages. Although benthic flow and solute fluxes are known to have strong impacts on fate and transport of oil deposited within marine sediments, their endogenous mechanisms still remain to be uncovered. In this paper, simulations of flow and solute transport processes along with hydrocarbon biodegradation were conducted in a cylindrical benthic chamber system to investigate influences of benthic hydrodynamics on oil biodegradation in permeable marine sediments. Results show that ripple-flow interactions create subsurface recirculation cells whereby seawater infiltrates into the benthic sediments at ripple troughs while groundwater discharges near the crests. It results in a spatially varied oil biodegradation rate in marine sediments. Significant oil biodegradation occurs near sediment ripple troughs due to direct oxygen recharge, while biodegradation of oil deposited uphill becomes slow due to limited oxygen replenishment. Oil biodegradation decreases subsurface oxygen content, and consequently impedes discharge of oxygen from benthic sediments. Our results reveal a dynamic interaction between oil biodegradation and benthic flow and solute transport processes, which has strong implications for predicting oil persistence and biodegradation within marine sediments and its associated impacts on benthic biogeochemical processes.

* Corresponding author at: Genwest Systems, Inc, Edmonds, WA 98020, USA.
E-mail address: leo.geng@noaa.gov (X. Geng).

https://doi.org/10.1016/j.jhazmat.2022.129211
Received 31 March 2022; Received in revised form 7 May 2022; Accepted 19 May 2022
Available online 25 May 2022

1. Introduction

Oil spills pose severe threats to marine coastal areas worldwide, deteriorating shoreline environments and causing severe ecological and economic damage. The 1989 Exxon Valdez oil spill contaminated around 800 km of shorelines within Prince William Sound, Alaska (Michel and Hayes, 1999; Short et al., 2004; Boufadel et al., 2016). In 2002, the Prestige oil spill occurred off the coast of Galicia, Spain, polluting over 600 sandy beaches along the Spanish Atlantic coast (Fernández-Fernández et al., 2011; Acosta-González et al., 2015). The 2010 Deepwater Horizon oil spill led to the release of an estimated 3.19 million barrels of crude oil into the Gulf of Mexico and an estimated 22, 000 tons of weathered oil washed up on northern Gulf of Mexico beaches (Michel et al., 2013; Boufadel et al., 2014; Geng et al., 2021a). Incidents of these magnitudes resulted in serious consequences on marine ecosystems, degrading abundance and diversity of benthic communities (Glemarec and Hussenot, 1981; Teal and Howarth, 1984). The toxicity in oils is primarily from aromatic hydrocarbons, particularly polycyclic aromatic hydrocarbons (PAHs) (Neff, 2002). Marine organisms are found to be affected by PAHs at every life stage, from free floating embryos and larvae to sexually mature adults (Adzigbli and Yuewen, 2018), and across species types. For instance, crustaceans can be exposed to oil through digging into oiled sediments, ingestion with food, and direct interaction (Cormack et al., 2011; Montagna et al., 2013), and often experience high mortality after oil spills (McCay et al., 2001). Bodkin et al. (2012) reported consequent impacts of the Exxon Valdez oil spill on the decrease in sea otter subpopulation rate in the heavily oiled northern Knight Island area of Prince William Sound. Reuscher et al. (2017) investigated impacts of the Deepwater Horizon oil spill on benthic infauna of the northern Gulf of Mexico continental slope. Their study found that oil originating from the Deepwater Horizon reached the seafloor and had a persistent negative impact on diversity of soft-bottom, deep-sea benthic communities. While signs of recovery for some benthic community variables are shown, full recovery had not yet occurred even four years after the spill.

There are various driving mechanisms that can cause sedimentation of spilled oil onto nearshore and benthic sediments (Teal and Howarth, 1984; Boufadel et al., 2019). Mixing of spilled oil with sediments often occurs in shallow water by breaking waves and further transport to deeper water is driven by subsequent currents (Fig. 1A) (Owens and Lee, 2003; O'Laughlin et al., 2017). Oil could also attach onto particulate matter suspended in the water column and subsequently sink in deeper water (Gong et al., 2014; Shan et al., 2020). Pore-water advection within marine sediments is often generated by the pressure gradients at the sediment surface that occur when bottom current flow is deflected by topographical structures such as mounds or ripples (Huettel and Gust, 1992; Janssen et al., 2005a). It has been proven to play a critical role in biogeochemical processes in marine benthic sediments, including carbon mineralization, nutrient recycling, and recycled primary production (Janssen et al., 2005a; Geng et al., 2021b). Tracer studies illustrated that ripple-flow interactions generate groundwater recirculation cells in marine sediments with flows infiltrating in the ripple troughs and exfiltrating from crests (Fig. 1B) (Webb and Theodor, 1968; Shum, 1992). Such seawater-groundwater recirculation brings organic matter and oxygen into the sediment, creates horizontal concentration gradients that can be as strong as the vertical gradients, and provides an important mechanism for enhancing mineralization of organic matter in marine sediments (Huettel et al., 1998). Although advective flow and solute fluxes across the water-sediment interface could have strong impacts on fate and transport of oil deposited within marine sediments, endogenous mechanisms of benthic flow and solute exchange interacting with oil biodegradation in marine sediments have not been investigated yet.

Investigation of benthic flow and solute exchange has been widely performed with benthic chambers. Experiments involve benthic stirred chambers where the centrifugal-force-induced pressure gradients at the sediment surface generate pore-water advection that circulates the overlying water through the sediment (Tengberg et al., 1995; Glud et al., 1996), and benthic landers deployed to the sea floor for direct in-situ measurements and observations (Black et al., 2001; D'Onghia et al., 2018). Mathematical modeling has also been widely used to investigate flow and solute transport processes within benthic sediments. It allows us to interpret measurement data collected from experiments and examine complex field-like conditions which are difficult to reproduce with laboratory experiments. Khalili et al. (1997), (1999) derived a numerical solution of the Darcy-Brinkmann-Lapwood equation to characterize the axisymmetric advective flow in a cylindrical chamber system. Calculations were performed to quantify the flow exchange between the permeable sediment and the overlying water. Meysman et al. (2007) conducted numerical simulations to investigate biologically and physically induced flow and tracer dynamics in marine benthic sediments. In their study, the finite element package COMSOL Multiphysics™ 3.2a was used to develop flow and reactive transport models for characterizations of advective flow and associated fluxes across the sediment-water interface. While considerable efforts have been made on modeling benthic flow and solute exchange processes, interactions between coastal benthic exchange dynamics and oil biodegradation have not been numerically conducted within benthic oil-contaminated sediments.

The objective of this paper is to investigate interactions between benthic oil biodegradation and pore-water advection along with solute exchange in marine sediments. We developed a two-dimensional (2D) flow and reactive transport model in cylindrical coordinates for the investigation. The development was based on transformation of our prior developed BIOMARUN model from Cartesian to cylindrical coordinates. We conducted simulations of groundwater flow, reactive transport of oxygen and a nutrient (nitrogen), and hydrocarbon biodegradation in a cylindrical benthic sediment chamber to

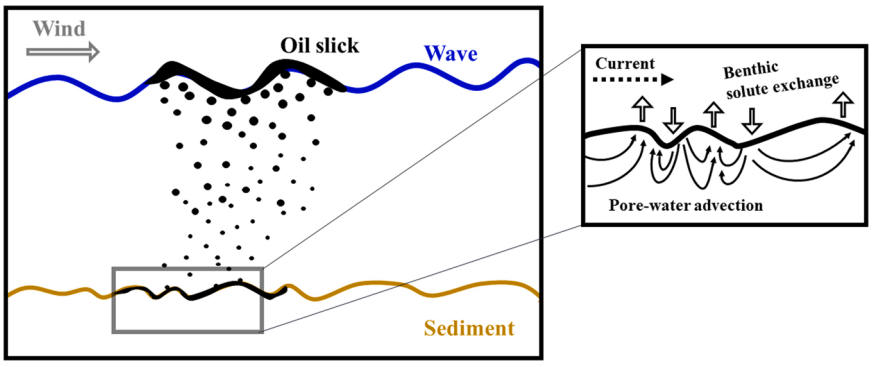

Fig. 1. Schematic of oil deposition and benthic exchange processes within permeable marine sediments. Note that the pressure gradients generated by ocean currents over ripples create circulation cells in marine sediments with flows infiltrating in the ripple troughs and exfiltrating from crests.

characterize the patterns of microbial degradation of oil subjected to benthic flow and solute flux exchange across the water-sediment interface. Particle tracking was further performed to analyze advective flow paths and associated travel time in this chamber system. The results highlight the important role of benthic hydrodynamics in hydrocarbon biodegradation within permeable marine sediments.

2. Methods

2.1. BIOMARUN model in cylindrical coordinates

The BIOMARUN model in Cartesian coordinates has been developed and validated in our prior studies (Geng et al., 2015, 2016, 2017a). The model couples the MARUN model (Boufadel et al., 1999; Geng and Boufadel, 2017; Geng et al., 2020), a 2-D finite element model considering density-dependent flow and solute transport in variably saturated media, with the BIOB model, a multiplicative Monod model for hydrocarbon biodegradation (Geng et al., 2013, 2014a). In this paper, we transformed the BIOMARUN model from Cartesian coordinates to cylindrical coordinates, named CYL-BIOMARUN, to simulate benthic flow and solute transport processes in a cylindrical chamber system. The equation for the conservation of water is written as:

$$\frac{\partial(\beta\phi S)}{\partial t}=\frac{1}{r}\frac{\partial\left(r\beta K_r\frac{\partial\psi}{\partial r}\right)}{\partial r}+\frac{\partial\left(\beta K_z\frac{\partial\psi}{\partial z}\right)}{\partial z}+\frac{\partial\left(\beta^2 K_z\right)}{\partial z}, \tag{1}$$

where β is the density ratio [-] defined as the ratio of salt-dependent water density to freshwater density [ML^{-3}]; ϕ is porosity [-], S is soil moisture ratio [-], ψ is pressure head [L], and K_r and K_z are radial and vertical freshwater hydraulic conductivities.

The conservative solute (e.g., salt) transport equation can be expressed as:

$$\phi S\frac{\partial c_0}{\partial t}=\beta\phi S\frac{\left(D_{rr}\frac{\partial c_0}{\partial r}+D_{rz}\frac{\partial c_0}{\partial z}\right)}{r}+\beta\nabla\cdot\left(\phi S\overrightarrow{D}\cdot\nabla c_0\right)-\overrightarrow{q}\cdot\nabla c_0, \tag{2}$$

where c_0 is concentration, and $\overrightarrow{q}$ is Darcy flux vector given by:

$$\overrightarrow{q}=\left(q_r,q_z\right)=-\left(K_r\frac{\partial\psi}{\partial r},K_z\frac{\partial\psi}{\partial z}+\beta\right), \tag{3}$$

The term $\overrightarrow{D}$ represents physical dispersion tensor written as

$$\overrightarrow{D}=\frac{1}{\|\overrightarrow{q}\|}\begin{pmatrix}\alpha_L q_r^2+\alpha_T q_z^2 & (\alpha_L-\alpha_T)q_r q_z\\ (\alpha_L-\alpha_T)q_r q_z & \alpha_T q_r^2+\alpha_L q_z^2\end{pmatrix}, \tag{4}$$

where $\|\overrightarrow{q}\|=\sqrt{q_r^2+q_z^2}$, α_L and α_T are longitudinal and transverse dispersivities (L), respectively.

The reactive solute transport equation can be expressed as:

$$\phi SR_i\frac{\partial c_i}{\partial t}=\beta\phi S\frac{\left(D_{rr}\frac{\partial c_i}{\partial r}+D_{rz}\frac{\partial c_i}{\partial z}\right)}{r}+\beta\nabla\cdot\left(\phi S\overrightarrow{D}\cdot\nabla c_i\right)-\overrightarrow{q}\cdot\nabla c_i+\phi DR_i r_i, \tag{5}$$

where R_i is the retardation coefficient of i_{th} solute c_i; r_i is a reaction rate representing generation or consumption. Six reactive components of two types of oil components (alkanes and polycyclic aromatic hydrocarbons (PAHs)), their corresponding microbial degraders, dissolved oxygen and a nutrient (nitrogen) are considered. The reaction network of these six components is consistent with the BIOB model, where in general microbes consume dissolved oxygen and nutrients for degrading oil compounds following modified Monod kinetics. For example, the growth coefficient of microbial degraders, μ_i, can be expressed as follows:

$$\mu_i=\mu_{\max}\left(1-\frac{X_i}{X_{\max}}\right)\left(\frac{S_i}{K_S+S_i}\right)\left(\frac{N}{K_N+N}\right)\left(\frac{O^4}{K_O+O^4}\right), \tag{6}$$

Where $i=1$ and 2, denoting alkane and PAH degraders, respectively, and $\mu_{\max}$ represents maximum growth coefficients (day^{-1}). The parameters S_i, N, and O represent concentrations of substrate, nutrient, and oxygen. The parameters K_S and K_N represent the half-saturation concentrations for substrate and nitrogen, respectively (see Geng et al., 2014a and (2015) for details). The CYL-BIOMARUN model was validated by reproducing the experimental results measured in Khalili et al. (1999) (Fig. 2).

2.2. Numerical simulations of oil biodegradation in a benthic chamber system

The simulated domain was constructed in a cylindrical coordinate system with the radius length of 50 cm and height of 100 cm, representing a cylindrical benthic chamber system. A mesh of 2278 nodes (34 nodes in the radial and 67 nodes in the vertical) was used, resulting in ~1.5 cm spatial resolution. The mesh was made fine enough to meet the criterion for the grid Peclet number to be less than or equal to 2.0 (Zheng and Bennett, 2002). For the flow simulation, a steady-state radial-symmetric pressure distribution was applied at the top boundary of the domain (Fig. 3A). This boundary condition is commonly used for simulating the chamber system where the sediment-water interface is flat, and a radial-symmetric stirring pattern establishes in the overlaying water (Glud et al., 1996). For fate and transport simulations, a Dirichlet boundary condition was used at the top boundary, and a Neumann boundary condition with zero dispersive flux was assigned to the rest of the boundaries. The initial concentration of dissolved oxygen and nutrients was assumed to be 6.0 mg/L and 1.0 mg/L in sediments, and 1.2 mg/L and 0.2 mg/L in seawater, respectively. To model microbial degradation of oil, the oil composition can be modeled as pseudo-components with distinct mass fractions and biodegradation rate (Thrift-Viveros et al., 2015). For simplification, the oil was assumed to be composed of two major groups, long-chain alkanes and polycyclic aromatic hydrocarbons (PAHs), deposited within the top 5 cm of sediments. The concentrations of alkanes and PAHs were assigned as 4.0 mg/kg of sediment and 2.0 mg/kg of sediment, respectively (Fig. 3B).

For all the simulations, the numerical model was first run for approximately 100 days without oil deposition until the hydraulic and hydrodynamic regime reached a steady state. The pressure and solute distributions were then used as initial conditions for the simulation with oil contamination near the sediment surface, which ran over a simulation time of 300 days. The time step was selected at 10.0 s, resulting in a grid Courant number less than 0.9 (a value less than 1.0 is required). The parameter values adopted in the simulations are reported in Table 1. Backward particle tracking was performed to reveal the flow pathways and associated travel time. A particle tracking code, named NEMO-3D, based on the random walk particle tracking algorithm was used (Geng et al., 2014b, 2017b, 2020). The neutrally buoyant particles were released at a 5-cm interval along the sediment surface, driven by the flow fields obtained from the CYL-BIOMARUN simulation.

3. Results

3.1. Comparison with the experiment data of Khalili et al. (1999)

Khalili et al. (1999) conducted experiments to investigate recirculating flow through benthic fluid-sediment interfaces. The experimental set-up is a stationary cylinder that contains a fluid-saturated porous medium with supernatant water on top. The recirculating flow was generated by deploying a rotating lid in the upper fluid region, and further characterized by monitoring dye washout from the sediment.

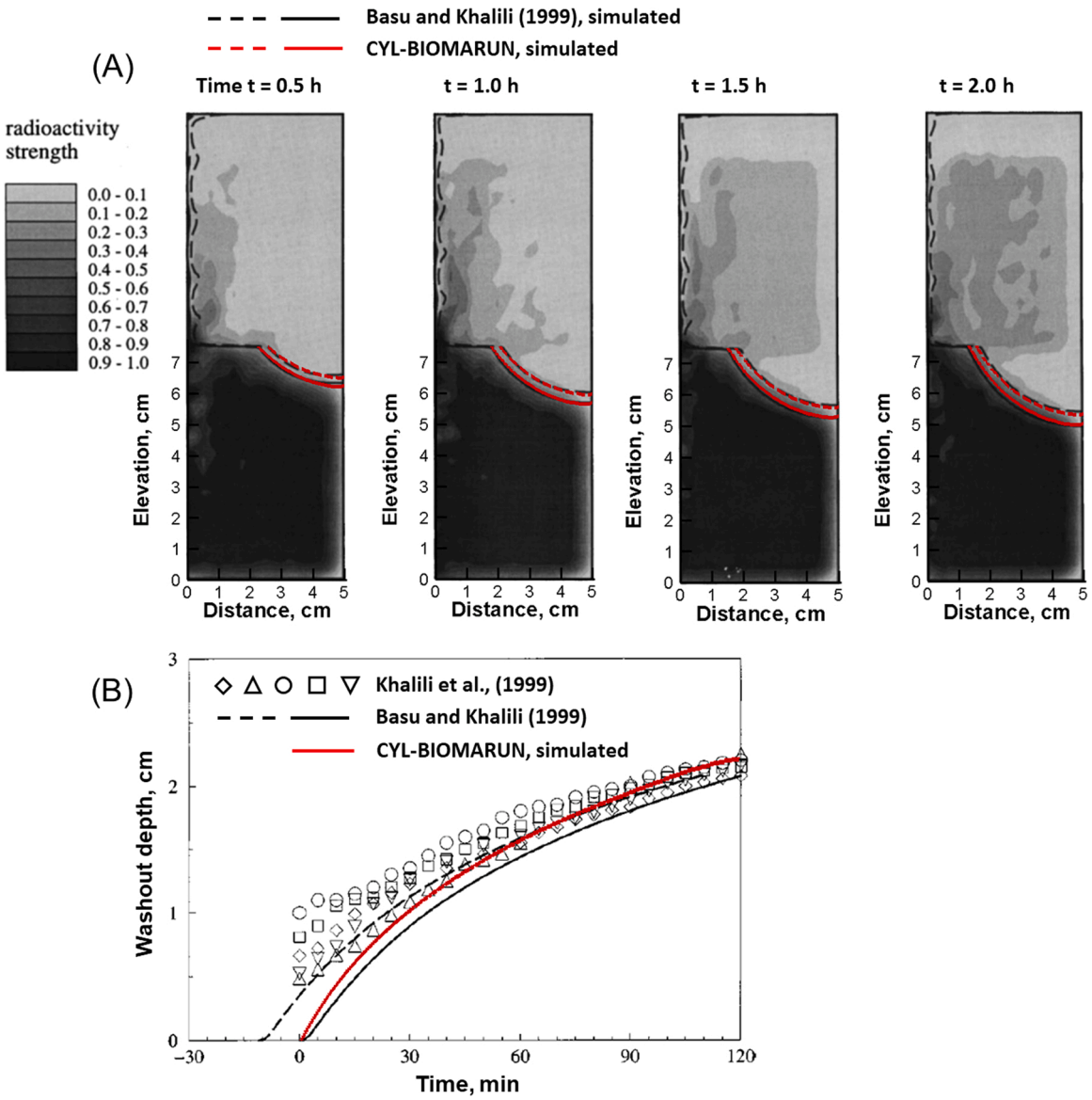

Fig. 2. (A) a comparison of normalized radioactivity strength measured by PET (gray-scale filled contours) in Khalili et al. (1999) with numerical results obtained from Basu and Khalili (1999) and CYL-BIOMARUN model at different times. The dashed and solid curves represent the simulated radioactivity of 0.5 and 0.9, respectively. (B) A comparison of washout depths obtained from experiments and numerical simulations. Note that in order to compensate for the effect of premixing (i.e., observed loss of some dye from the sediment to the fluid layer at the initial instant of the experiments) in the experiments, Khalili et al. (1999) shifted back their numerical results by 12 min for additional comparison, plotted as a dashed line.

Dye transport was visualized using positron emission tomography (PET), a non-invasive technique which allows to see through an opaque solid matrix, and to obtain full 3-D pictures of washing out dye from the sediment. In their study, digital photographic visualization and associated image processing were also performed to further quantify the near-wall dye-washout depth. Fig. 2 A shows a comparison of normalized radioactivity strength measured at different times by PET along with numerical results obtained by CYL-BIOMARUN model and the model developed in Basu and Khalili (1999). As shown in the figure, the CYL-BIOMARUN model reasonably captures the dye transport within the sediment column. The results of washout depth show that both numerical models underestimate the first half-hour washout of dye from the sediment (Fig. 2B). This is most likely due to the loss of some dye from the sediment to the fluid layer when the experiments were initialized, which was not considered in the numerical simulations.

3.2. Simulations of pore-water advection, solute exchange, and oil biodegradation in a benthic chamber system

Surface pressure gradients have a strong influence on flow and transport processes within benthic sediments. Fig. 3A shows that the pressure gradients imposed along the sediment surface alter subsurface pressure distribution, creating a high-pressure zone at the outer ring of the chamber and relatively low-pressure zone in the proximity of the chamber center. The resulting pressure differences transmit through the subsurface and generate pressure gradients in both radial and vertical directions. The penetration depth is approximately 20 cm for the simulations considered in this paper. Fig. 3C and D show that an upper plume is generated in the subsurface with seawater-derived chemical properties that are distinguished from ambient groundwater. This is expected as the formation of the plume is due to seawater infiltration. The plume has a deeper expansion beneath the high-pressure zone, and becomes shallower as it moves to the relatively low-pressure zone. The

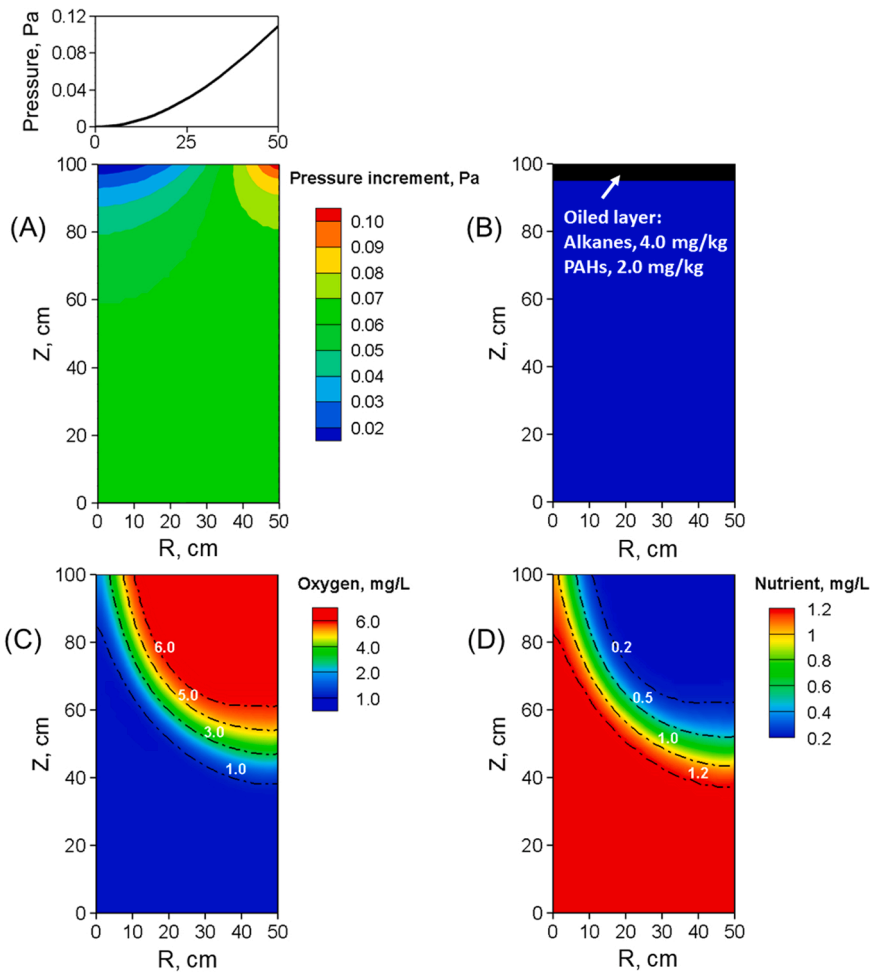

Fig. 3. Simulated steady-state distributions of (A) pressure, (C) dissolved oxygen, and (D) nutrient (i.e., nitrogen) in the benthic chamber system. (B) Initial oil (i.e., alkanes and PAHs) distribution in the benthic sediment. In Fig. 3A, the upper panel shows the pressure distribution along the water-sediment interface, and the lower panel shows steady-state pressure increment (above 100 cm) built by pressure gradients imposed at the water-sediment interface.

Table 1
Parameter values used in the numerical simulations.

	Value	Unit
Physical parameters		
Hydraulic conductivity, K	180	cm/h
Porosity, ϕ	0.39	-
Longitudinal dispersivity, α_L	3.0	cm
Transverse dispersivity, α_T	0.3	cm
Microbial parameters*		
Alkanes		
Initial microbial concentration, X_B	0.06	mg/kg
Maximum microbial concentration, X_{max}	0.63	mg/kg
Maximum growth rate, μ_{max}	0.71	d^{-1}
Half-saturation concentration for substrate consumption, K_S	228.03	mg/kg
Half-saturation concentration for nitrogen consumption, K_N	0.7	mg/L
Microbial growth dependence on oxygen, K_O	2.0	mg/L
PAHs		
Initial microbial concentration, X_B	0.0006	mg/kg
Maximum microbial concentration, X_{max}	0.57	mg/kg
Maximum growth rate, μ_{max}	2.47	d^{-1}
Half-saturation concentration for substrate consumption, K_S	46.13	mg/kg
Half-saturation concentration for nitrogen consumption, K_N	0.49	mg/L
Microbial growth dependence on oxygen, K_O	2.0	mg/L

* The microbial parameter values are obtained and calibrated in Geng et al. (2014a) and 2015.

concentration of oxygen gradually decreases from 6.0 mg/L to 1.0 mg/L and concentration of nutrients gradually increases from 0.2 mg/L to 1.2 mg/L in the proximity of the plume edge, indicating substantial mixing between seawater and groundwater in benthic sediments. The steady-state simulations show the maximum washout depth by seawater is ~20 cm while the thickness of the seawater-groundwater mixing zone is ~25 cm.

Particle tracking results show the pressure gradients create a recirculation cell whereby seawater infiltrates into the benthic sediments through the high-pressure zone and groundwater discharge occurs along the low-pressure zone (Fig. 4). Fig. 4 A shows the advective flow pathways within the recirculation cell simulated by a backward particle tracking scheme. Infiltration flow occurs near the outer ring of the chamber between R = 40 cm and 50 cm, while exfiltration flow is present at the inner part of the chamber between R = 0 and 40 cm. The particles migrating along deeper flow paths experience longer travel time (Fig. 4B). In particular, the travel time of the particles discharged near the location of R = 2 cm is about 100 years. The particles' travel time drops exponentially as their discharge locations get close to the infiltration zone due to shorter flow paths.

Oil biodegradation demonstrates a large spatial variation in benthic sediments. The concentration contour of alkanes shows that two biodegradation hotspots appear in the oiled sediment layer after 30 days near the top within the infiltration zone and near the bottom within the exfiltration zone, respectively (Fig. 5A). The spatial extent of these two hotspots gradually expands with time (e.g., time t = 60 days and 100

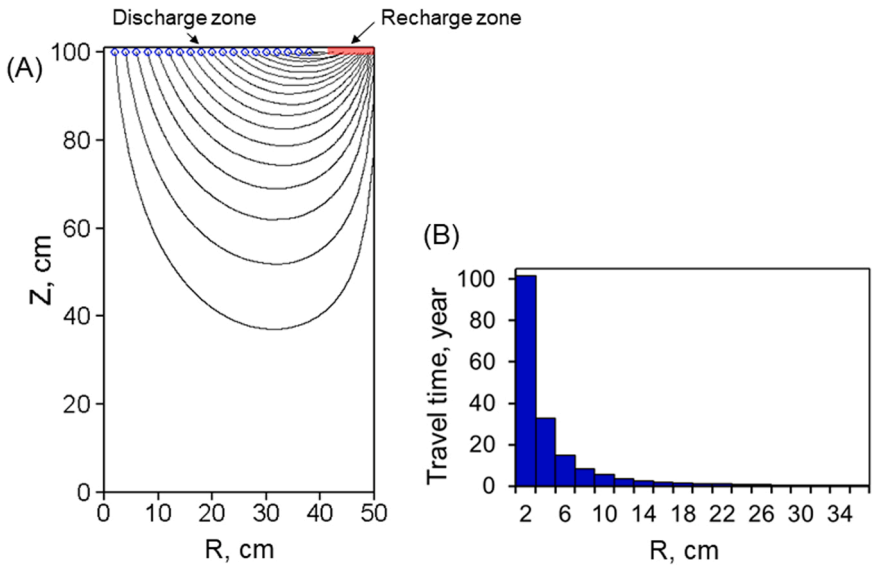

Fig. 4. (A) Simulated flow paths of the particles released at 0.1-m interval along the sediment surface from R = 2–50 cm. (B) Travel time of the particles. Note that backward particle tracking was used to track advective flow paths. The start and end locations of particle flow paths are marked with blue symbols and a red line, respectively.

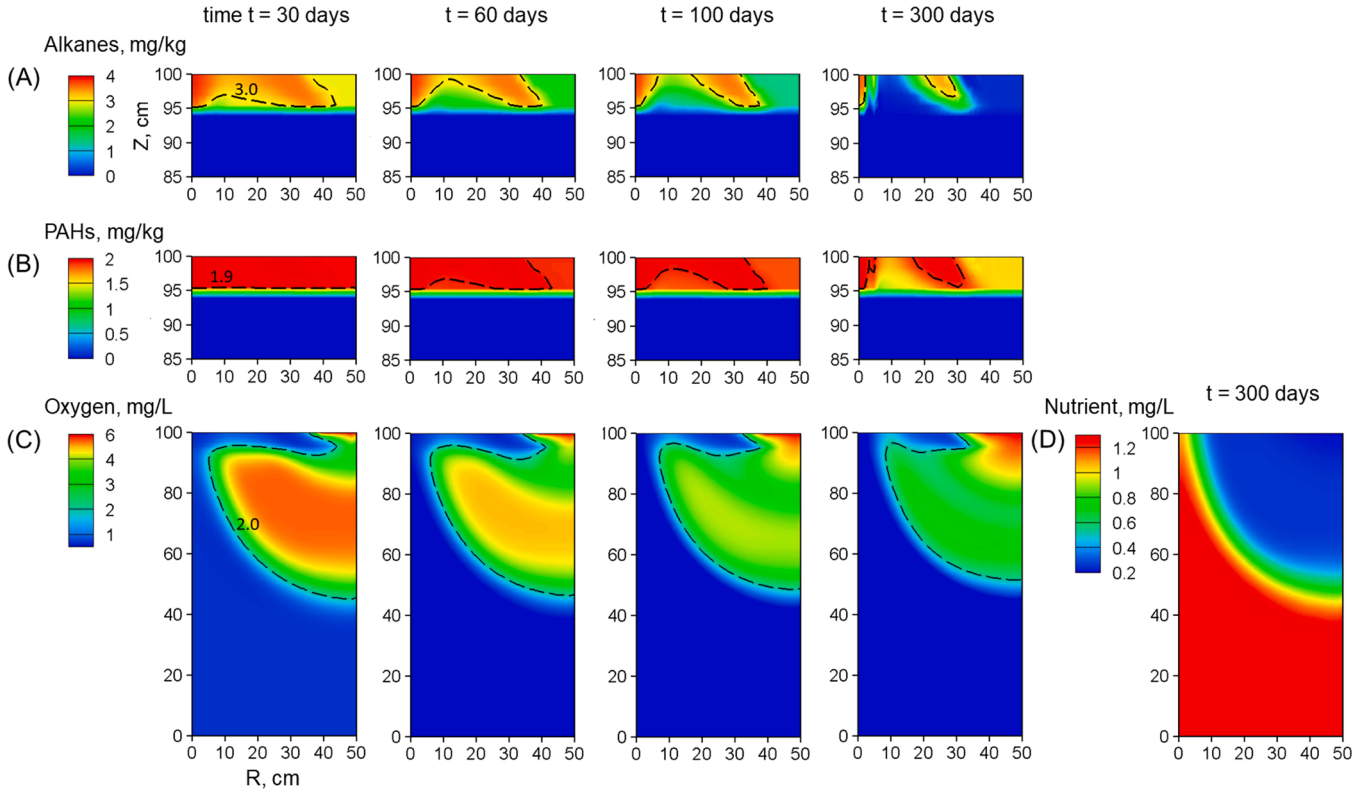

Fig. 5. Simulated concentration contours of (A) alkanes, (B) PAHs, (C) oxygen, and (D) nutrient at different times. The dashed contour lines for alkanes and PAHs represent 75% and 95% of its initial concentration, respectively. The threshold of 2.0 mg/L that supports aerobic oil biodegradation is marked in oxygen contours. The nutrient contours demonstrate a negligible change with time; therefore, only its 300-day concentration contour is shown herein.

days). After 300 days, nearly all the alkanes deposited within these two hotspots are biodegraded. In contrast, a considerable amount of alkanes still remains near the middle ring of the chamber. Similar tempo-spatial patterns are observed for PAHs as well but at much lower biodegradation rate (Fig. 5B). Compared to alkanes, biodegradation of PAHs is negligible within the first 100 days. After 300 days, biodegradation of PAHs is around 15% near its hotspots, and negligible at other locations.

Oil biodegradation greatly alters benthic oxygen conditions (Fig. 5C). After 30 days, the near-surface oxygen level significantly drops within the exfiltration zone to a concentration less than 1.0 mg/L, resulting in anoxic conditions for oil biodegradation. The oxygen level beneath the oiled sediment layer gradually decreases with time, due to large oxygen consumption from the upper oiled layer. In contrast, the oxygen content within the infiltration zone always remains above 2.0 mg/L, which

provides a favorable aerobic condition for oil biodegradation. This is most likely because direct recharge of oxygen-rich seawater to some extent compensates for the oxygen consumption there. Compared to oxygen, the nutrient (nitrogen) condition remains at its original level. This is probably due to recycling of nutrients during the oil biodegradation processes (Fig. 5D). On the one hand, oil degraders consume nitrogen for microbial growth, but on the other hand, they release nitrogen during their endogenous decay.

Fig. 6A reports the alkane biodegradation at three different radial locations. As expected, the highest biodegradation rate is observed at the outer ring of the chamber (i.e., R = 45 cm), where above 98% of alkanes are biodegraded after 300 days. The biodegradation rate tends to be lower as it moves to the inner side (i.e., R = 15 cm), where alkanes are biodegraded about 80% after 300 days. The lowest alkane biodegradation occurs near the mid-ring location (i.e., R = 30 cm); nearly 10% of alkanes are biodegraded within the first 20 days, and then the biodegradation rate dramatically drops. Similar tempo-spatial patterns are also observed for PAHs at a much lower rate. This is consistent with tempo-spatial variation of oxygen level within the benthic sediment (Fig. 6 C). The oxygen concentration demonstrates a sudden decrease after the oil deposition. In particular, the oxygen concentration drops below 2 mg/L at locations R = 15 cm and 30 cm, indicating anoxic environments there for oil biodegradation. In contrast, oxygen concentration at location R = 45 cm only drops down to 4.5 mg/L and then recovers back to 5.5 mg/L after 300 days.

Fig. 7 reports the percentage (%) loss of alkanes and PAHs at different radial locations. Obviously, the % loss is the largest near the outer ring of the chamber (i.e., between R = 40 cm and 50 cm), which is about 100% and 20% for alkanes and PAHs, respectively. Comparable loss of alkanes and PAHs is found at the zone between R = 5 cm and 15 cm. The % loss drops as it moves to the middle ring of the chamber, reaching the minimum at R = 30–35 cm, which is about 35% and 5% for alkanes and PAHs, respectively. The minimum loss is also observed at the center of the chamber (i.e., between R = 0 and 5 cm), which is probably due to persistent low oxygen content there.

Pore-water advection significantly affects oil biodegradation in benthic sediments. The pore-water velocity contour shows a higher magnitude near the surface at the outer and inner ring of the chamber (Fig. 8A). Interestingly, it is inconsistent with the magnitude of pressure imposed at the sediment surface, which gradually decreases along the radial direction from the outer ring boundary to the inner center of the chamber. This is due to the fact that the intensity of pore-water flow is determined by the pressure gradient rather than pressure itself. Fig. 8B and C show exchange flux and flow across the sediment surface,

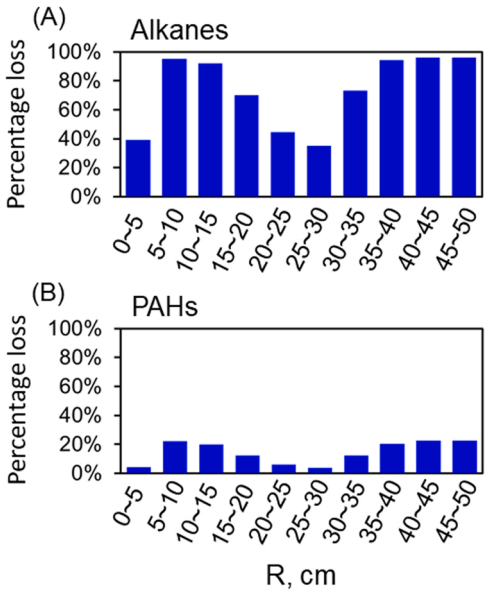

Fig. 7. Percentage loss of (A) alkanes and (B) PAHs at different radial locations.

respectively. Seawater infiltration occurs near the outer ring of the chamber between R = 40 cm and 50 cm, showing the largest rate at the chamber edge. In contrast, groundwater discharge occurs at the inner part of the chamber between R = 0–40 cm, reaching the highest rate at R = 25 cm. Although the majority of groundwater discharge appears near the middle ring of the chamber, discharge flux tends to be the largest near the inner center of the chamber (i.e., R = 5 cm), and gradually decreases as the radius increases. It indicates a relatively poor hydraulic exchange at the middle ring of the chamber, which to some extent explains the relatively low oil biodegradation rate there.

The interactions between benthic solute exchange and biodegradation of deposited oil in benthic sediments are dynamic. Fig. 9A shows the temporospatial evolution of oxygen exchange across the water-sediment interface after the oil deposition. Although there is a steady oxygen recharge into the benthic sediments, the oxygen exchange curves tend to be flat at 0.0 mg/h along the entire discharge zone following the oil deposition (e.g., at time t = 10 days and 100 days). It indicates that oil deposition impedes discharge of oxygen from the benthic sediments due to its large consumption for hydrocarbon biodegradation. The positive discharge of oxygen starts to occur again after 300 days of the oil

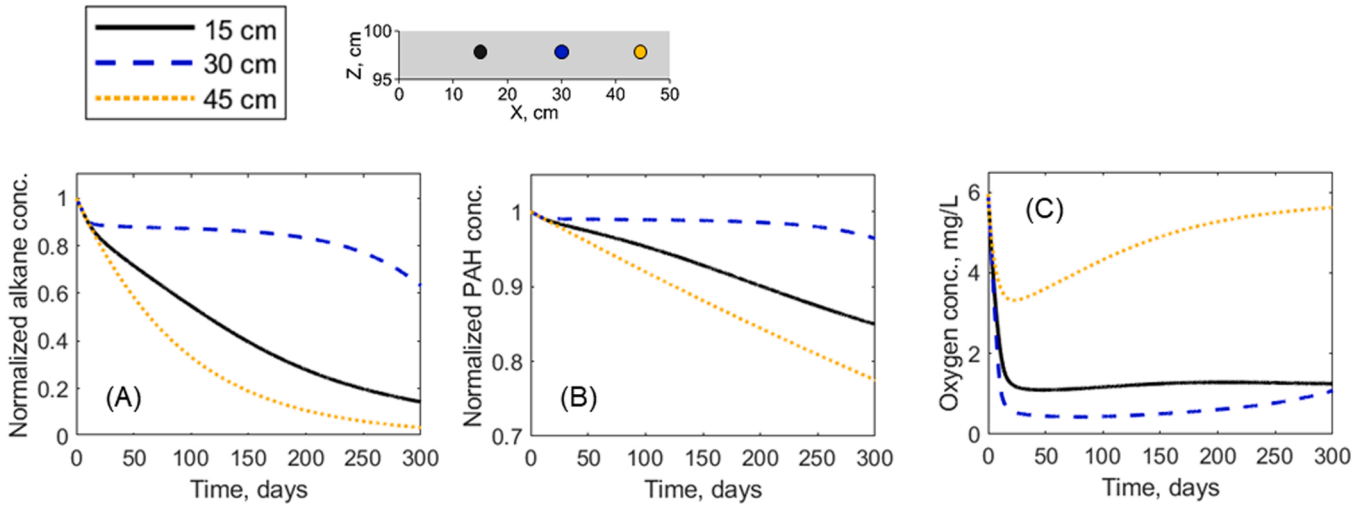

Fig. 6. Temporal change of concentration for (A) alkanes, (B) PAHs, and (C) dissolved oxygen at three different radial locations (Z = 97.5 cm, and R = 15 cm, 30 cm, and 45 cm). The output locations are marked in the upper panel using the same color as the concentration curves.

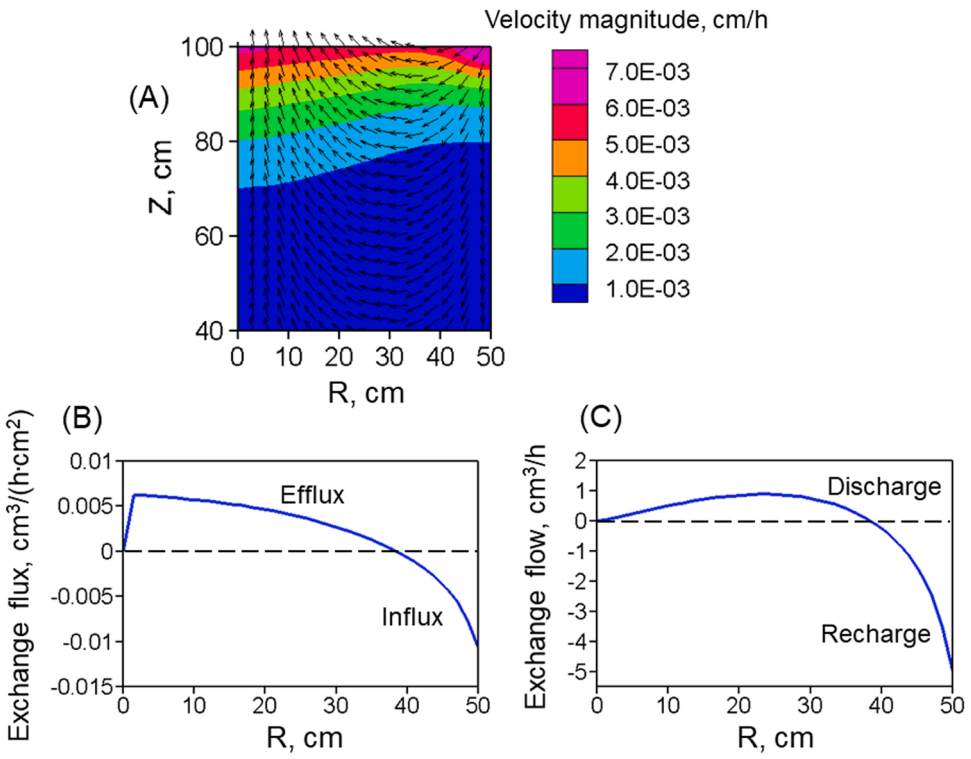

Fig. 8. (A) Simulated pore-water velocity field. The spatial distribution of (B) exchange flux ($cm^3/h \cdot cm^2$) and (C) exchange flow (cm^3/h) along the sediment-water interface. In Fig. 8 A, the color contour and uniform vectors represent magnitude and direction of pore water flow, respectively.

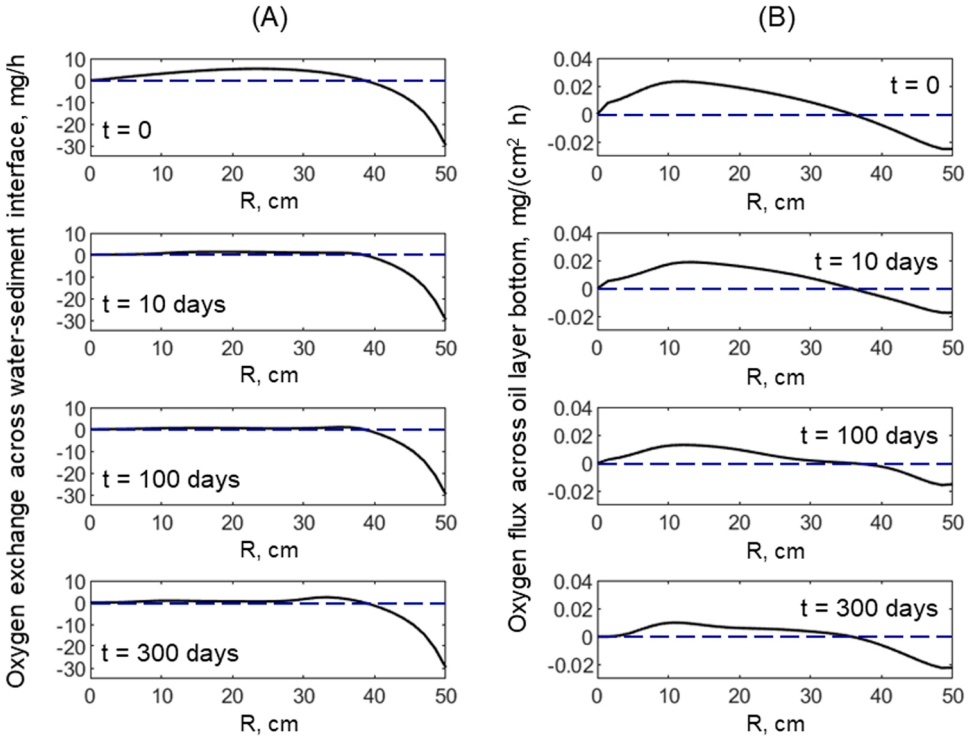

Fig. 9. (A) Oxygen exchange across the water-sediment interface. (B) Oxygen flux across bottom of the oiled layer (i.e., Z = 95 cm). Note that the positive and negative values represent upward and downward flow directions, respectively.

deposition at locations between R = 30 cm and 40 cm which is in proximity of the oxygen recharge zone. It indicates that the oxygen concentration is returned to its initial levels by seawater infiltration after major amounts of oil are removed by biodegradation along the discharge flow paths. Fig. 9B shows the temporospatial evolution of oxygen flux at the bottom of the oiled layer (i.e., Z = 95 cm). The oxygen replenishment along the entire bottom of the oiled sediment layer largely decreases within the first 100 days following the deposition, particularly

next to the infiltration zone between R = 30 cm and 40 cm. This is due to the oxygen consumption at the infiltration zone, diminishing the replacement of oxygen downstream. Such oxygen depletion has lesser impacts on farther discharge locations (e.g., between R = 5 cm and R = 30 cm) due to the following reasons: 1) initial oxygen storage within benthic sediments provides additional oxygen replenishment for downstream oil biodegradation, and 2) the higher water and oxygen flux at the farther discharge locations. The intensity of oxygen replenishment is consistent with the magnitude of oil biodegradation within the benthic sediments, indicating the importance of solute (i.e., oxygen) exchange in biodegradation of deposited oil in benthic sediments.

4. Discussion

Our results reveal a significant role of benthic flow advection and solute exchange in the fate of oil deposited within permeable marine sediments. Pore-water advection has been recognized as one of the most important drivers for benthic biogeochemical processes (Janssen et al., 2005b; Cook et al., 2007; Rocha, 2008). Our simulation results indicate that bottom current flows deflected by topographical sediment structures will create subsurface pore-water recirculation cells whereby seawater infiltrates into sediment ripple troughs while groundwater discharges near the crest. It leads to a dynamic hydraulic and biogeochemical environment for hydrocarbon biodegradation in benthic sediments. At sediment troughs, the determinants of oil biodegradation rate are infiltration rate and biogeochemical properties of seawater, while biodegradation of oil deposited near the sediment crest is primarily controlled by upwelling groundwater flux beneath the exfiltration zone. Therefore, oil deposited within marine sediments demonstrates spatially different biodegradation rates. Faster oil biodegradation occurs in sediment ripple troughs due to direct and sufficient oxygen recharge by seawater infiltration. In contrast, biodegradation of oil deposited uphill is slow and even anoxic (i.e., extremely slow). Such spatial variations will increase the level of challenge to assess oil spill contamination in marine sediments solely based on field measurements. This is because random selection of oil-contaminated sediment samples might cause large variability of oil measurements as natural attenuation of oil behaves differently in marine sediments, depending on local topographic and flow patterns. Our results suggest that characterization of sediment topographic properties and hydraulic conditions at sampling locations are essential for thorough data interpretation and assessment of oil spills contaminating marine sediments.

Dissolved oxygen and nutrients are key factors affecting hydrocarbon biodegradation; limited availability of either could slow down the biodegradation rate considerably (Passow and Overton, 2021; Wang et al., 2021). It has been observed that dissolved oxygen concentration affects aerobic microbial growth in a sharp way (Borden and Bedient, 1986; Borden et al., 1986; Chiang et al., 1989). The optimal oxygen concentration for microbial activities to support aerobic oil biodegradation is 2.0–3.0 mg/L, above which increasing the oxygen concentration does not enhance the microbial activities. However, when the concentration drops below 2.0 mg/L, microbial activity switches sharply from aerobic to anaerobic in a way that dramatically decreases oil biodegradation rate. Seawater infiltration into marine sediments has been found to provide a major source of dissolved oxygen that enhances sedimentary respiration as well as hydrocarbon biodegradation (Anschutz et al., 2009; Santos et al., 2009). Our results demonstrate that pore-water advection provides a critical control on benthic solute (e.g., oxygen and nutrients) exchange. Ripple-flow interactions generate an oxygen-rich plume beneath the benthic sediment surface, which has strong implications on the fate and biodegradation of oil deposited in marine sediments. It likely creates an oxygen-rich environment (i.e., above 2 mg/L) at ripple troughs that is favorable for aerobic oil biodegradation. In contrast, oil biodegradation becomes slow and even anoxic near the ripple crests because of the fact that oxygen is primarily consumed by oil biodegradation near the recharge zone (i.e., ripple troughs) which reduces downstream oxygen replenishment. Our results also show that oil deposition restructures benthic oxygen conditions. Oil biodegradation reduces subsurface oxygen content, and consequently impedes discharge of oxygen from the water-sediment interface. Such change could have long-term impacts on benthic microbial community structures which have a large potential to alter nitrogen dynamics, especially inorganic nitrogen release and denitrification processes (Giblin et al., 1995; Werner et al., 2006).

5. Conclusion

In this paper, we conducted numerical simulations of flow and solute transport processes and hydrocarbon biodegradation in a cylindrical benthic chamber system to investigate influences of benthic flow and solute exchange on oil biodegradation in marine sediments. Our results show that ripple-flow interactions create subsurface recirculation cells whereby seawater infiltrates into the benthic sediments through ripple troughs while groundwater discharges near ripple crests. It leads to spatially varied oil biodegradation rate in marine sediments, depending on local topographic and flow patterns. Significant oil biodegradation will occur in sediment ripple troughs due to direct and sufficient oxygen recharge by seawater infiltration. In contrast, biodegradation of oil deposited uphill is slow and under anoxic condition where oxygen replenishment is prohibited. Overall, this study reveals endogenous mechanisms within permeable benthic sediments that affect persistence and biodegradation of the deposited oil. It highlights the importance of benthic flow advection and solute exchange on characterizing fate of oil after its deposition within marine sediments. In particular, benthic flow recirculation along with solute exchange (e.g., oxygen and nutrients) creates a highly dynamic environment that increases spatial variability of oil decomposition within marine sediments. In coastal environments, permeability of sediments is heterogeneous, which could strongly alter magnitude and pathways of pore-water flows. In addition, relatively low temperature and high pressure in deep ocean could play an important role in benthic oil biodegradation there. These factors are not considered in current work, which are essential and need to be included in future studies.

Environmental implication

Spilled oils have been recognized as among the worst kinds of hazardous materials, causing severe coastal ecological and economic damages. Although benthic flow and solute fluxes are known to have strong impacts on fate and transport of oil deposited within marine sediments, their endogenous mechanisms still remain to be uncovered. To fill such research gap, we conducted numerical simulations of flow and solute transport processes along with hydrocarbon biodegradation in a cylindrical benthic chamber system. Our results reveal/ interpret the endogenous mechanisms that affect the persistence and biodegradation of deposited oil within permeable benthic marine sediments.

CRediT authorship contribution statement

Xiaolong Geng: Conceptualization, Methodology, Writing – orignal draft. **Christopher H. Barker:** Supervision, Methodology, Reviewing. **Amy MacFadyen:** Supervision, Reviewing, Editing. **Michel C Boufadel:** Methodology, Model Development, Data analysis. **Kenneth Lee:** Supervision, Methodology, Draft Editing. **Dalina L. Thrift-Viveros:** Writing, Reviewing, Editing, **Robert Jones:** Validation, Reviewing, and Editing. **Caitlin O'Connor:** Validation, Reviewing, and Editing.

Declaration of Competing Interest

The authors declare that they have no known competing financial interests or personal relationships that could have appeared to influence the work reported in this paper.

Acknowledgment

This work was funded by the United States National Science Foundation (Division of Earth Sciences [EAR] Grant ID: #2130595. However, it does not necessarily reflect the views of the funding agency, and no official endorsement should be inferred.

References

Acosta-González, A., Martirani-von Abercron, S.-M., Rosselló-Móra, R., Wittich, R.-M., Marqués, S., 2015. The effect of oil spills on the bacterial diversity and catabolic function in coastal sediments: a case study on the Prestige oil spill. Environ. Sci. Pollut. Res. 22 (20), 15200–15214.

Adzigbli, L., Yuewen, D., 2018. Assessing the impact of oil spills on marine organisms. J. Oceanogr. Mar. Res 6 (179), 472–479.

Anschutz, P., Smith, T., Mouret, A., Deborde, J., Bujan, S., Poirier, D., Lecroart, P., 2009. Tidal sands as biogeochemical reactors. Estuar., Coast. Shelf Sci. 84 (1), 84–90.

Basu, A., Khalili, A., 1999. Computation of flow through a fluid-sediment interface in a benthic chamber. Phys. Fluids 11 (6), 1395–1405.

Black, K.S., Fones, G.R., Peppe, O.C., Kennedy, H.A., Bentaleb, I., 2001. An autonomous benthic lander:: Preliminary observations from the UK BENBO thematic programme. Cont. Shelf Res. 21 (8–10), 859–877.

Bodkin, J.L., Ballachey, B.E., Coletti, H.A., Esslinger, G.G., Kloecker, K.A., Rice, S.D., Reed, J.A., Monson, D.H., 2012. Long-term effects of the 'Exxon Valdez'oil spill: sea otter foraging in the intertidal as a pathway of exposure to lingering oil. Mar. Ecol. Prog. Ser. 447, 273–287.

Borden, R.C., Bedient, P.B., 1986. Transport of dissolved hydrocarbons influenced by oxygen-limited biodegradation: 1. Theor. Dev., *Water Resour. Res.* 22 (13), 1973–1982.

Borden, R.C., Bedient, P.B., Lee, M.D., Ward, C.H., Wilson, J.T., 1986. Transport of dissolved hydrocarbons influenced by oxygen-limited biodegradation: 2. Field Appl., Water Resour. Res. 22 (13), 1983–1990.

Boufadel, M., Geng, X., An, C., Owens, E., Chen, Z., Lee, K., Taylor, E., Prince, R.C., 2019. A review on the factors affecting the deposition, retention, and biodegradation of oil stranded on beaches and guidelines for designing laboratory experiments. Curr. Pollut. Rep. 1–17.

Boufadel, M.C., Abdollahi-Nasab, A., Geng, X., Galt, J., Torlapati, J., 2014. Simulation of the landfall of the Deepwater Horizon oil on the shorelines of the Gulf of Mexico. Environ. Sci. Technol. 48 (16), 9496–9505.

Boufadel, M.C., Geng, X., Short, J., 2016. Bioremediation of the Exxon Valdez oil in Prince William sound beaches. Mar. Pollut. Bull. 113 (1–2), 156–164.

Boufadel, M.C., Suidan, M.T., Venosa, A.D., 1999. A numerical model for density-and-viscosity-dependent flows in two-dimensional variably saturated porous media. J. Contam. Hydrol. 37 (1–2), 1–20.

Chiang, C., Salanitro, J., Chai, E., Colthart, J., Klein, C., 1989. Aerobic biodegradation of benzene, toluene, and xylene in a sandy aquifer—data analysis and computer modeling. Groundwater 27 (6), 823–834.

Cook, P.L., Wenzhöfer, F., Glud, R.N., Janssen, F., Huettel, M., 2007. Benthic solute exchange and carbon mineralization in two shallow subtidal sandy sediments: effect of advective pore-water exchange. Limnol. Oceanogr. 52 (5), 1943–1963.

Cormack, C.D., Hale, J.A., Gabriel, J.J., Langman, O., 2011. Nasima and Oil–Do They Mix? Assessing Crab Survival in Oiled Sediments, paper presented at Proceedings international oil spill conference. API,, Washington, DC.

D'Onghia, G., Capezzuto, F., Carlucci, R., Carluccio, A., Maiorano, P., Panza, M., Ricci, P., Sion, L., Tursi, A., 2018. Using a benthic lander to explore and monitor vulnerable ecosystems in the Mediterranean Sea. Acta Imeko 7 (2), 45–49.

Fernández-Fernández, S., Bernabeu, A., Bouchette, F., Rey, D., Vilas, F., 2011. Beach morphodynamic influence on long-term oil pollution: The Prestige oil spill. J. Coast. Res. 890–893.

Geng, X., Abou Khalil, C., Prince, R.C., Lee, K., An, C., Boufadel, M.C., 2022a. Hypersaline pore water in Gulf of Mexico beaches prevented efficient biodegradation of Deepwater Horizon beached oil. Environ. Sci. Technol. 55 (20), 13792–13801.

Geng, X., Boufadel, M.C., 2017. The influence of evaporation and rainfall on supratidal groundwater dynamics and salinity structure in a sandy beach. Water Resour. Res. 53 (7), 6218–6238.

Geng, X., Boufadel, M.C., Cui, F., 2017a. Numerical modeling of subsurface release and fate of benzene and toluene in coastal aquifers subjected to tides. J. Hydrol. 551, 793–803.

Geng, X., Boufadel, M.C., Lee, K., Abrams, S., Suidan, M., 2015. Biodegradation of subsurface oil in a tidally influenced sand beach: Impact of hydraulics and interaction with pore water chemistry. Water Resour. Res. 51 (5), 3193–3218.

Geng, X., Boufadel, M.C., Personna, Y.R., Lee, K., Tsao, D., Demicco, E.D., 2014a. BioB: a mathematical model for the biodegradation of low solubility hydrocarbons. Mar. Pollut. Bull. 83 (1), 138–147.

Geng, X., Boufadel, M.C., Rajaram, H., Cui, F., Lee, K., An, C., 2020. Numerical study of solute transport in heterogeneous beach aquifers subjected to tides. Water Resour. Res. 56 (3) e2019WR026430.

Geng, X., Boufadel, M.C., Wrenn, B., 2013. Mathematical modeling of the biodegradation of residual hydrocarbon in a variably-saturated sand column. Biodegradation 24 (2), 153–163.

Geng, X., Boufadel, M.C., Xia, Y., Li, H., Zhao, L., Jackson, N.L., Miller, R.S., 2014b. Numerical study of wave effects on groundwater flow and solute transport in a laboratory beach. J. Contam. Hydrol. 165, 37–52.

Geng, X., Heiss, J.W., Michael, H.A., Boufadel, M.C., 2017b. Subsurface flow and moisture dynamics in response to swash motions: effects of beach hydraulic conductivity and capillarity. Water Resour. Res. 53 (12), 10317–10335.

Geng, X., Heiss, J.W., Michael, H.A., Li, H., Raubenheimer, B., Boufadel, M.C., 2022b. Geochemical fluxes across the land-sea interface through sandy coastlines: modulation due to major physical stressors and geological heterogeneity. Earth-Sci. Rev. 221, 103800.

Geng, X., Pan, Z., Boufadel, M.C., Ozgokmen, T., Lee, K., Zhao, L., 2016. Simulation of oil bioremediation in a tidally influenced beach: spatiotemporal evolution of nutrient and dissolved oxygen. J. Geophys. Res.: Oceans 121 (4), 2385–2404.

Giblin, A.E., Foreman, K.H., Banta, G.T., 1995. Biogeochemical Processes and Marine Benthic Community Structure: Which Follows Which? (edited). Linking Species & Ecosystems. Springer, pp. 37–44 (edited).

Glemarec, M., and E. Hussenot (1981), Définition d'une succession écologique en milieu meuble anormalement enrichi en matières organiques à la suite de la catastrophe de l'AMOCO CADIZ, paper presented at Proceedings of International Symposium on the Amoco Cadiz, Fate and Effects of the Oil Spill. CNEXO, Brest, France.

Glud, R.N., Forster, S., Huettel, M., 1996. Influence of radial pressure gradients on solute exchange in stirred benthic chambers. Mar. Ecol. Prog. Ser. 141, 303–311.

Gong, Y., Zhao, X., Cai, Z., O'reilly, S., Hao, X., Zhao, D., 2014. A review of oil, dispersed oil and sediment interactions in the aquatic environment: influence on the fate, transport and remediation of oil spills. Mar. Pollut. Bull. 79 (1–2), 16–33.

Huettel, M., Gust, G., 1992. Solute release mechanisms from confined sediment cores in stirred benthic chambers and flume flows. Mar. Ecol. Prog. Ser. Oldendorf 82 (2), 187–197.

Huettel, M., Ziebis, W., Forster, S., Luther Iii, G., 1998. Advective transport affecting metal and nutrient distributions and interfacial fluxes in permeable sediments. Geochim. Et. Cosmochim. Acta 62 (4), 613–631.

Janssen, F., Faerber, P., Huettel, M., Meyer, V., Witte, U., 2005a. Pore-water advection and solute fluxes in permeable marine sediments (I): calibration and performance of the novel benthic chamber system Sandy. Limnol. Oceanogr. 50 (3), 768–778.

Janssen, F., Huettel, M., Witte, U., 2005b. Pore-water advection and solute fluxes in permeable marine sediments (II): Benthic respiration at three sandy sites with different permeabilities (German Bight, North Sea). Limnol. Oceanogr. 50 (3), 779–792.

Khalili, A., Basu, A., Huettel, M., 1997. A non-Darcy model for recirculating flow through a fluid-sediment interface in a cylindrical container. Acta Mech. 123 (1), 75–87.

Khalili, A., Basu, A., Pietrzyk, U., Jørgensen, B.B., 1999. Advective transport through permeable sediments: a new numerical and experimental approach. Acta Mech. 132 (1), 221–227.

McCay, D.P. F., C.-A. Manen, M. Gibson, J. Catena (2001), Quantifying the Scale of Restoration Required to Compensate for the Impacts of the North Cape Oil Spill on Fish and Invertebrates, paper presented at International Oil Spill Conference, American Petroleum Institute.

Meysman, F.J., Galaktionov, O.S., Cook, P.L., Janssen, F., Huettel, M., Middelburg, J.J., 2007. Quantifying biologically and physically induced flow and tracer dynamics in permeable sediments. Biogeosciences 4 (4), 627–646.

Michel, J., Hayes, M.O., 1999. Weathering patterns of oil residues eight years after the Exxon Valdez oil spill. Mar. Pollut. Bull. 38 (10), 855–863.

Michel, J., Owens, E.H., Zengel, S., Graham, A., Nixon, Z., Allard, T., Holton, W., Reimer, P.D., Lamarche, A., White, M., 2013. Extent and degree of shoreline oiling: Deepwater Horizon oil spill, Gulf of Mexico, USA. PloS One 8 (6), e65087.

Montagna, P.A., Baguley, J.G., Cooksey, C., Hartwell, I., Hyde, L.J., Hyland, J.L., Kalke, R.D., Kracker, L.M., Reuscher, M., Rhodes, A.C., 2013. Deep-sea benthic footprint of the Deepwater Horizon blowout. PloS One 8 (8), e70540.

Neff, J.M., 2002. Bioaccumulation in Marine Organisms: Effect of Contaminants from Oil Well Produced Water. Elsevier.

O'Laughlin, C.M., Law, B.A., Zions, V.S., King, T.L., Robinson, B., Wu, Y., 2017. Settling of dilbit-derived oil-mineral aggregates (OMAs) & transport parameters for oil spill modelling. Mar. Pollut. Bull. 124 (1), 292–302.

Owens, E.H., Lee, K., 2003. Interaction of oil and mineral fines on shorelines: review and assessment. Mar. Pollut. Bull. 47 (9–12), 397–405.

Passow, U., Overton, E.B., 2021. The complexity of spills: the fate of the Deepwater Horizon oil. Annu. Rev. Mar. Sci. 13, 109–136.

Reuscher, M.G., Baguley, J.G., Conrad-Forrest, N., Cooksey, C., Hyland, J.L., Lewis, C., Montagna, P.A., Ricker, R.W., Rohal, M., Washburn, T., 2017. Temporal patterns of Deepwater Horizon impacts on the benthic infauna of the northern Gulf of Mexico continental slope. PloS One 12 (6), e0179923.

Rocha, C., 2008. Sandy sediments as active biogeochemical reactors: compound cycling in the fast lane. Aquat. Microb. Ecol. 53 (1), 119–127.

Santos, I.R., Burnett, W.C., Dittmar, T., Suryaputra, I.G., Chanton, J., 2009. Tidal pumping drives nutrient and dissolved organic matter dynamics in a Gulf of Mexico subterranean estuary. Geochim. Et. Cosmochim. Acta 73 (5), 1325–1339.

Shan, J., Wang, J., Zhan, J., Liu, L., Wu, F., Wang, X., 2020. Sorption behaviors of crude oil on polyethylene microplastics in seawater and digestive tract under simulated real-world conditions. Chemosphere 257, 127225.

Short, J.W., Lindeberg, M.R., Harris, P.M., Maselko, J.M., Pella, J.J., Rice, S.D., 2004. Estimate of oil persisting on the beaches of Prince William Sound 12 years after the Exxon Valdez oil spill. Environ. Sci. Technol. 38 (1), 19–25.

Shum, K., 1992. Wave-induced advective transport below a rippled water-sediment interface. J. Geophys. Res.: Oceans 97 (C1), 789–808.

Teal, J.M., Howarth, R.W., 1984. Oil spill studies: a review of ecological effects. Environ. Manag. 8 (1), 27–43.

Tengberg, A., De Bovee, F., Hall, P., Berelson, W., Chadwick, D., Ciceri, G., Crassous, P., Devol, A., Emerson, S., Gage, J., 1995. Benthic chamber and profiling landers in

oceanography—a review of design, technical solutions and functioning. Prog. Oceanogr. 35 (3), 253–294.
Thrift-Viveros, D.L., R. Jones, M. Boufadel (2015), Development of a new oil biodegradation algorithm for NOAA's oil spill modelling suite (GNOME/ADIOS), paper presented at Proceedings of the Thirty-Eighth AMOP Technical Seminar, Vancouver, BC, Canada.
Wang, S., Wang, D., Yu, Z., Dong, X., Liu, S., Cui, H., Sun, B., 2021. Advances in research on petroleum biodegradability in soil. Environ. Sci.: Process. Impacts 23 (1), 9–27.
Webb, J.E., Theodor, J., 1968. Irrigation of submerged marine sands through wave action. Nature 220 (5168), 682–683.
Werner, U., Bird, P., Wild, C., Ferdelman, T., Polerecky, L., Eickert, G., Jonstone, R., Hoegh-Guldberg, O., de Beer, D., 2006. Spatial patterns of aerobic and anaerobic mineralization rates and oxygen penetration dynamics in coral reef sediments. Mar. Ecol. Prog. Ser. 309, 93–105.
Zheng, C., Bennett, G.D., 2002. Applied Contaminant Transport Modelling. John Wiley and Sons, New York, USA.